

FINITE ELEMENT MODELLING OF THE RESPONSE OF LONG FLOATING STRUCTURES UNDER HARMONIC EXCITATION

C. Georgiadis

SINTEF, The Foundation of Scientific
Industrial Research at the Norwegian Institute of Technology
Trondheim, Norway

ABSTRACT

The response of long floating structures to a harmonic excitation is the basis for the response calculation in a short crested wave field. This paper will present consistent formulas for obtaining the nodal loads in a finite element analysis. The accuracy of the method used is compared with the results obtained using a Rayleigh-Ritz approximation of the response with continuous eigenfunctions. The error of using an irrational finite element model is demonstrated for comparison, and to indicate to designers of similar structures the large effects which they may be overlooking.

INTRODUCTION

The usual method of calculating the response of long floating structures due to wave excitation is the frequency domain analysis. The modelling of the response to a harmonic oblique wave is the basis for this. The response to a wave field is obtained by the superposition of the responses to harmonic directional components with amplitudes obtained from the directional wave energy spectrum.

General purpose finite element programs are usually used for the response calculation. These programs do not provide methods for computing the nodal loads in the case of continuous harmonic oblique loading along the structure. An accurate computation of the nodal loads should take into account the amplitude and phase variations of the loading between the nodal points. It will be shown that even reasonably closely spaced nodal points cannot account for these effects.

This paper will present consistent formulas with the virtual work formulation of finite elements, along with ways to implement them in finite element programs. The accuracy of the method used is compared with the results of a Rayleigh-Ritz approximation of the response with continuous eigenfunctions, where the effects of discretizing the wave forces to nodal loads are not taking place.

PROBLEM FORMULATION AND NOMENCLATURE

The problem which will be dealt with here is the computation of nodal loads in the case of a long structure under a continuous harmonic oblique loading. The types of structures to which this applies are floating bridges or breakwaters in a wave field. The wave field is usually described by a directional wave spectrum (1,2)

$$S(\omega, \theta) = S(\omega) \Psi(\theta) \quad , \quad (1)$$

where $S(\omega)$ is the unidirectional wave spectral density (models like Pierson-Moskowitz, JONSWAP, Darbyshire-Scott) which gives the wave energy distribution for various frequencies; and $\Psi(\theta)$ is a spreading function (usual model $\Psi(\theta) = C \cos^n(\theta - \theta_0)$), which gives the angular distribution of the wave energy.

From the directional wave spectrum the sea state can be simulated as the superposition of harmonic components in different directions. If we assume that in the simulation we use N wave frequencies ($i=1,2,\dots,N$), and M wave directions ($j=1,2,\dots,M$), the sea state will be simulated with $K=N*M$ components of the form

$$\eta_{ij} = \zeta_{ij} \cos(\omega_i t + \phi_{ij}) \quad , \quad (2)$$

where the amplitude is obtained from the directional wave spectrum as

$$\zeta_{ij} = \sqrt{S(\omega_i, \theta_j) \Delta\omega \Delta\theta} \quad . \quad (3)$$

There are many ways of choosing the frequencies ω_i in the simulation process and ref.(2) shows some of the methods available. The angles θ_j can be chosen equally spaced from $-\pi/2$ to $+\pi/2$. In Eq.(2) ϕ_{ij} are random phase angles between 0 and 2π . In Eq.(3) $\Delta\omega$ and $\Delta\theta$ are wave frequency and wave direction intervals around ω_i and θ_j .

The response of the structure to a short crested sea described by a directional wave spectrum is obtained as the superposition of the responses to the individual harmonic components η_{ij} . Each harmonic

component of the loading is characterized by a loading or wave frequency ω_i and a direction θ_j in respect to the axis of the structure (Fig.1). For the rest of the discussion as we deal only with one harmonic component the subscripts i and j will be dropped and we will use ω and θ for the loading frequency and direction.

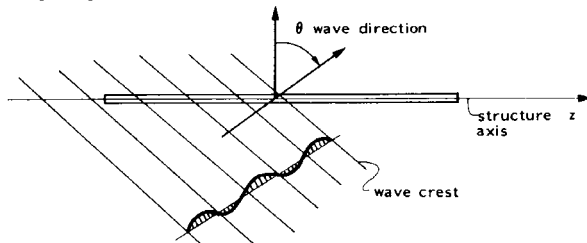


FIG.1 GEOMETRICAL DEFINITIONS

Troughout this paper linear wave theory is assumed. The loading along the structure (Fig.1) for a harmonic wave at angle θ is

$$f(z,t) = \delta e^{i(\mu z - \omega t)} \quad (4)$$

where δ is a dimensional (force/unit length) hydrodynamic coefficient (4,5), and depends on the wave frequency and direction. For deep water conditions we have

$$\mu = \kappa \sin \theta = \frac{2\pi}{\lambda} \sin \theta = \frac{\omega^2}{g} \sin \theta \quad (5)$$

where κ and λ are the wave number and the wave length.

REYLEIGH-RITZ APPROXIMATION

A first approach in calculating the response of the structure is a Rayleigh-Ritz approximation, in which the response values are approximated with continuous functions. This approximation will be used as basis for checking the accuracy of the finite element model which is going to be discussed in the next section.

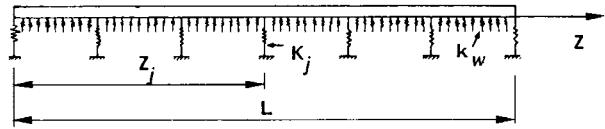
A general structural model is shown in Fig.(2). For simplicity in the analysis the structure is assumed to have constant cross section with stiffness EI , virtual mass m , and virtual damping $2\xi\omega m$. For the sway motion the anchor cables are modeled as elastic springs with stiffness K_j at locations z_j . For the heave and roll motion the structure behaves like a beam on elastic foundation, with foundation modulus equal to the buoyancy stiffness, $k_w = \rho_w g B$ for heave, and $k_w = \rho_w g B^3/12$ for roll. (B is the width of the rectangular cross section, ρ_w and g are the specific mass of the water and the acceleration of gravity).

In the analysis the three directions of motion will be assumed uncoupled. This approximation is quite accurate for straight structures, as the coupling between the three directions of motion due to hydrodynamic effects is very small (6).

The Euler-Lagrange equations of the structural response, using q_i for generalized coordinates, are

$$\frac{d}{dt} \left(\frac{\partial E}{\partial \dot{q}_i} \right) = \frac{\partial E}{\partial q_i} - \frac{\partial F}{\partial q_i} \quad (6)$$

where $E=T-U$; T and U are the kinetic and potential energy of the system; F is the damping forces quadratic form.



Sway : $K_j = \text{cable stiffness}, k_w = 0$
 Heave : $K_j = 0, k_w = \rho_w g B$
 Roll : $K_j = 0, k_w = \rho_w g B^3/12$

FIG.2 GENERAL STRUCTURAL MODEL

We assume the structure displacements of the form

$$w(z,t) = \sum_{n=0}^{\infty} C_n(t) Y_n(z) \quad (7)$$

where $Y_n(z)$ is a complete set of functions satisfying the kinematic boundary conditions. One choice is the eigenfunctions derived from the solution of the beam vibration equation

$$\frac{d^4 Y(z)}{dz^4} = \left(\frac{\nu}{L}\right)^4 Y(z) \quad (8)$$

For a beam with free ends the solutions are (7)

$$Y_0\left(\frac{z}{L}\right) = 1 \quad (9a)$$

$$Y_1\left(\frac{z}{L}\right) = \sqrt{3} (1 - 2\frac{z}{L}) \quad (9b)$$

$$Y_{n+1}\left(\frac{z}{L}\right) = \cosh \nu_n \frac{z}{L} + \cos \nu_n \frac{z}{L} - \alpha_n (\sinh \nu_n \frac{z}{L} + \sin \nu_n \frac{z}{L}) \quad (9c)$$

$n = 1, 2, 3, \dots$

where ν_n is the solution of the transcendental equation

$$\cos \nu \cosh \nu = 1 \quad (10a)$$

and

$$\alpha_n = \frac{\cosh \nu_n - \cos \nu_n}{\sinh \nu_n - \sin \nu_n} \quad (10b)$$

Values of ν_n for $n = 1, 2, 3, 4, 5$, are 4.73004074, 7.85320462, 10.9956078, 14.1371655, 17.2787597, and $(2n+1)\pi/2$ for $n > 5$.

These functions are orthogonal to each other

$$\int_0^L Y_n(z) Y_m(z) dz = \begin{cases} L & \text{for } n=m \\ 0 & \text{for } n \neq m \end{cases} \quad (11a)$$

$$\int_0^L (Y_{n+1}''(z))^2 dz = \left(\frac{\nu_n}{L}\right)^4 L \quad \text{for } n=1, 2, 3, \dots \quad (11b)$$

$$\int_0^L (Y_n''(z))^2 dz = 0 \quad \text{for } n=0, 1 \quad (11c)$$

Expressing the quantities in Eq.(6) using the functions $Y_n(z)$ of Eq.(7) we obtain:

Kinetic energy

$$T = \int_0^L \left(\frac{m}{2}\right) [\dot{w}(z,t)]^2 dz = \frac{mL}{2} \sum_{n=0}^{\infty} [\dot{C}_n(t)]^2 \quad (12a)$$

Potential energy

$$\begin{aligned}
 U &= \int_0^L \frac{EI}{2} [w''(z,t)]^2 dz + \int_0^L \frac{k_w}{2} [w(z,t)]^2 dz \\
 &+ \sum_{j=1}^M \frac{K_j}{2} [w(z_j,t)]^2 - \int_0^L f(z,t) w(z,t) dz \\
 &= \frac{1}{2} EIL \sum_{n=0}^{\infty} \left(\frac{v_n}{L}\right)^4 [C_n(t)]^2 + \frac{1}{2} k_w L \sum_{n=0}^{\infty} [C_n(t)]^2 \\
 &+ \frac{1}{2} \sum_{j=1}^M K_j \sum_{n=0}^{\infty} \sum_{l=0}^{\infty} C_n(t) C_l(t) Y_n(z_j) Y_l(z_j) \\
 &- \sum_{n=0}^{\infty} C_n(t) \int_0^L f(z,t) Y_n(z) dz ; \quad (12b)
 \end{aligned}$$

Damping quadratic form

$$F = \int_0^L \frac{1}{2} (2\xi\omega m) [\dot{w}(z,t)]^2 dz = \frac{1}{2} (2\xi\omega m) L \sum_{n=0}^M [\dot{C}_n(t)]^2. \quad (12c)$$

Using

$$C_n(t) = C_n e^{-i\omega t}, \quad (13a)$$

$$g_{n1j} = Y_n(z_j) Y_1(z_j), \quad (13b)$$

$$f(z,t) = \delta e^{i\mu z} e^{-i\omega t}, \quad (13c)$$

$$B_n = \delta \int_0^L e^{i\mu z} Y_n(z) dz, \quad (13d)$$

and Eq.(12.a,b,c), from Eq.(6) we obtain the equations of motion

$$\begin{aligned}
 &[-mL\omega^2 + EIL\left(\frac{v_n}{L}\right)^4 + k_w L + 2\xi\omega^2 mL i] C_n \\
 &+ \sum_{l=0}^{\infty} \left(\sum_{j=1}^M K_j g_{n1j} \right) C_l = B_n \quad (14) \\
 &\text{for } n=0,1,2,3,\dots
 \end{aligned}$$

Eq.(14) represents a system of infinite number of equations for the unknown variables C_n . For practical applications a finite number of equations is used, and the system of equations becomes

$$\sum_{j=0}^N A_{ij} C_j = B_i \quad i=0,1,2,\dots,N. \quad (15)$$

Expressions for the complex variables A_{ij} and B_i are presented in ref.(6) and (8). The system of Eq.(15) is solved for the variables $C_i = c_j + i\delta_j$. The structure displacements and bending moments are computed as

$$w(z,t) = \text{Real} \left[\sum_{n=0}^N C_n Y_n(z) e^{-i\omega t} \right], \quad (16a)$$

$$M(z,t) = -EI \text{Real} \left[\sum_{n=0}^N C_n Y_n''(z) e^{-i\omega t} \right]. \quad (16b)$$

FINITE ELEMENT MODELLING

Setting up the finite element model of the structure is quite straight forward. Any finite

element program with beam elements can be used for the job. The point which needs attention and can introduce errors in the analysis, if it is treated irrationally, is the computation of the nodal loads.

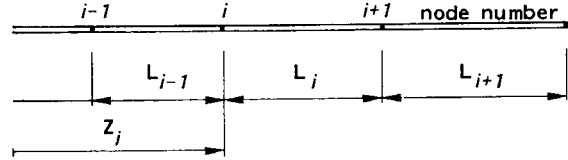


FIG.3 FINITE ELEMENT MODEL OF THE STRUCTURE

A first approach in computing the nodal loads is to compute the load characteristics at the nodal points, and assume that this loading is extended halfway to the adjacent nodes. Using the notation of Fig.(3), the nodal load at node i is

$$R_i(t) = \delta \left(\frac{L_i + L_{i-1}}{2} \right) \cos(\omega t + \phi_i) \quad (17)$$

where ϕ_i is the phase angle of the loading at the nodal point i in respect to the coordinate origin

$$\phi_i = \frac{2\pi z_i}{(\lambda/\sin\theta)} = \mu z_i \quad (18)$$

This way of modelling the nodal forces does not take into account the space-time variation of the loading between the nodal points, which affects the magnitude and the phase angle of the loading. A more accurate nodal load computation will reveal the error in the amplitude and the phase of the nodal loads.

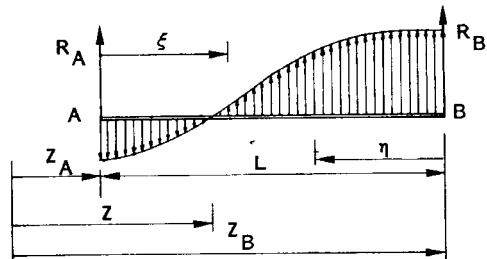


FIG.4 BEAM ELEMENT

Figure (4) shows a beam finite element subjected to a harmonic loading. Lets use $N_1(\xi)$ and $N_2(\eta)$ for the displacement functions along the beam element for unit displacements at nodes A and B. Applying the virtual work principle the nodal loads at A and B are computed as (9)

$$R_A(t) = \delta \int_0^L N_1(\xi) e^{i\mu(z_A+\xi)-i\omega t} d\xi, \quad (19)$$

$$R_B(t) = \delta \int_0^L N_2(\eta) e^{i\mu(z_B-\eta)-i\omega t} d\eta, \quad (20)$$

where z , z_A , z_B , ξ , and η are distances shown in Fig.(4).

Using, as a first approximation, linear displacement fields we get for the nodal loads

$$R_A(t) = \delta \epsilon L e^{i(\mu z_A + \psi - i\omega t)} = \delta \epsilon L e^{i(\phi_A + \psi) - i\omega t} \quad (21a)$$

$$R_B(t) = \delta \epsilon L e^{i(\mu z_B - \psi - i\omega t)} = \delta \epsilon L e^{i(\phi_B - \psi) - i\omega t} \quad (21b)$$

where ϕ_A and ϕ_B are phase angles computed from Eq.(18) at the points A and B

$$\phi_A = \mu z_A \quad (22a)$$

$$\phi_B = \mu z_B \quad (22b)$$

The amplitude and phase angle parameters ϵ and ψ are

$$\epsilon = \frac{\sqrt{2 + (\mu L)^2 - 2\cos(\mu L) - 2\mu L \sin(\mu L)}}{(\mu L)^2} \quad (23)$$

$$\psi = \arctan \left\{ \frac{\mu L - \sin(\mu L)}{1 - \cos(\mu L)} \right\} \quad (24)$$

It should be noticed that the parameter (μL) used in all the relations here is a nondimensional parameter depending on the wave length λ and direction θ , and the nodal point spacing (L)

$$\mu L = \kappa L \sin \theta = \frac{\omega^2}{g} L \sin \theta = \frac{2\pi L}{\lambda \sin \theta} \quad (25)$$

From Eq.(21,a,b), and the notation of Fig.(3) we obtain for the nodal load at node i

$$R_i(t) = \delta \left\{ \epsilon_{i-1} L_{i-1} \cos(\omega t + \phi_{i-1} - \psi_{i-1}) + \epsilon_i L_i \cos(\omega t + \phi_i + \psi_i) \right\} \quad (26)$$

where ϵ_i and ψ_i are computed for the span i using Eq.(23) and (24), and ϕ_i is computed for the node i using Eq.(18).

As we can see the parameters ϵ and ψ represent the amplitude and phase angle changes between Eq.(17) and (26). The way these parameters vary with the wave length and direction (parameter μL), is shown in Fig.(5) and (6). The variations can be considerable for high wave frequencies or very oblique angles with the structure axis.

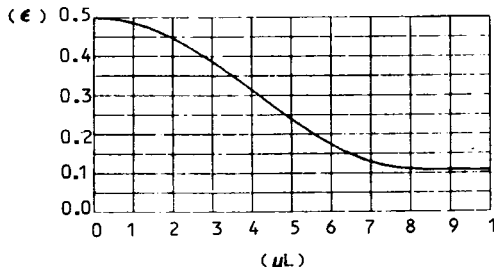


FIG.5 AMPLITUDE PARAMETER LINEAR DISPL. FIELD

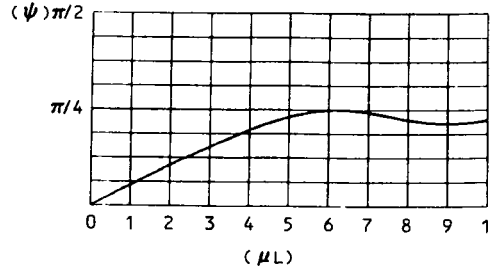


FIG.6 PHASE ANGLE PARAMETER LINEAR DISPL. FIELD

Figure (7) shows a more accurate computation of the nodal loads based on third degree polynomial approximation for the displacement functions.

APPLICATION CONCLUSIONS

Two methods have been presented for the modelling of the response to harmonic excitation. One is a Rayleigh-Ritz approximation, and the other is a finite element model. We will pay more attention to the finite element approach since it is used more often.

The Rayleigh-Ritz method approximates the response with continuous functions and thus can be considered very close to the true solution if the number of continuous functions (harmonics), which are used to approximate the response, is adequate enough. The right number of harmonics depends on the frequency of the excitation and can be established by looking at the improvement of the response values with the increase of the number of harmonics.

Three different levels of finite element approximation have been presented. The model of Eq.(17) uses simple tributary areas to determine the nodal loads, the model of Eq.(26) is based on linear displacement fields, and the formulas presented in Fig.(7) are based on a third degree polynomial approximation for displacement fields. The higher the order of the displacement field, which is used, the better the approximation is.

The poor level of approximation obtained by using Eq.(17) can be seen from the plots of the parameters ϵ and ψ (Fig.5, 6 and 7), which show the differences in the amplitude and the phase angle of the loading between the first and the two other finite element approximations. A usual way of improving the accuracy of a finite element approximation is to choose more close the nodal points. The error of using Eq.(17) instead of Eq.(26) can be considered negligible if the parameter ϵ is close to 0.5 and the parameter ψ is close to 0. From Fig(5) and (6) we can conclude that this can happen if $\mu L \ll 1$, which results in a critical nodal point distance L_c ($\mu L_c = 1$)

$$\frac{L_c}{\lambda} = \frac{1}{2\pi \sin \theta} \quad \text{or} \quad L_c = \frac{g T^2}{4\pi^2 \sin \theta} \quad (27)$$

Fig.(8) shows plots of the above critical nodal point distance for various frequencies and directions of the applied wave loading. As can be seen the nodal point distance should be chosen to be very small to reduce the error. This will have a considerable increase in the computational cost using the finite element model.

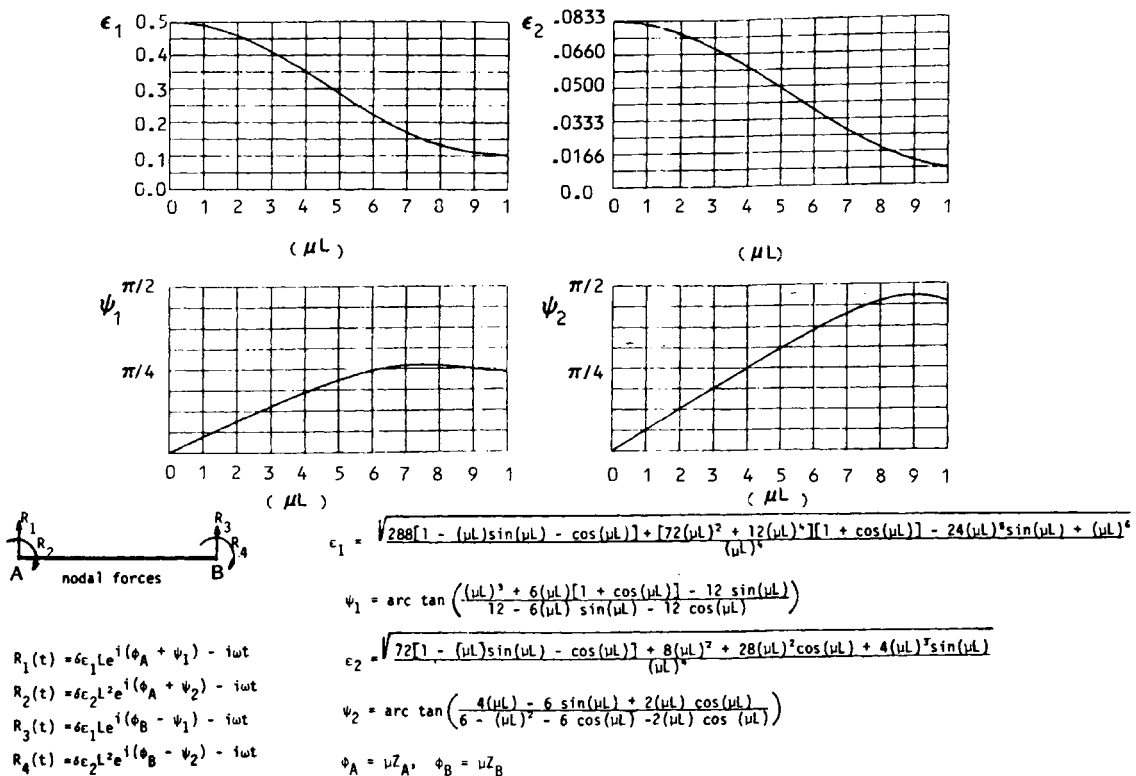


FIG. 7 THIRD DEGREE POLYNOMIAL FOR DISPLACEMENT FIELD

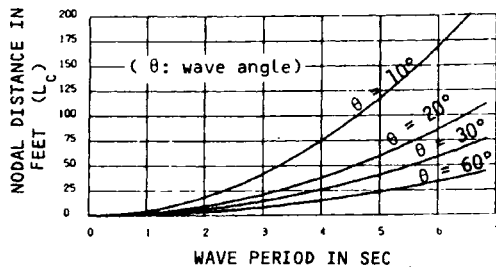


FIG. 8 CRITICAL NODAL POINT DISTANCE L_c

Using Eq.(17) and choosing an average nodal point distance to give accurate results for the mean wave frequency and direction of the loading, does not necessarily reduce the error for the overall response to a wave spectrum. As can be seen from Fig.(5) and (6) the deviation of ϵ from 0.5 and ψ from 0 increases considerably for high wave frequencies and very oblique waves (large values of μL). In the response evaluation in a short crested wave field, the contribution of the higher wave frequencies, and the oblique waves, can cause the final response values to be completely wrong.

In order to investigate better the accuracy of the finite element approximations a test structure was modelled. The basic properties of the structure were chosen to be close to the properties of the original Hood-Canal floating bridge (10). The structure has

been subjected to harmonic waves from three different directions (10,30, and 50 degrees with the structural axis), and the response has been evaluated for various wave frequencies. The results for the maximum displacements and bending moments for the heave motion are presented in the following figures. Fig.(9) shows a Rayleigh-Ritz approximation. Fig.(10) shows a finite element approximation with nodal loads computed using simple tributary areas. Fig.(11) shows a finite element approximation based on linear displacement field for the computation of the nodal loads. Fig.(12) shows a finite element approximation based on a third degree polynomial approximation for the displacement field. For the Rayleigh-Ritz approximation 24 harmonics have been used. The variation of the results between 12, 16, 20 and 24 harmonics has indicated that the results shown in Fig.(9) can be considered very close to the true response values. For the finite element models 21 nodal points have been used.

From the results shown for this test structure the order of approximation with the three finite element models is clear. Comparison between the response values shown in Fig.(10) and the response values shown in Figs.(9), (11) and (12) shows that the use of simple tributary areas for the calculation of the nodal loads results in completely unreasonable picture for the structural response.

The close response values shown in Fig.(9) and (12) recommend the use of a third degree polynomial approximation for the computation of the nodal loads in a finite element model.

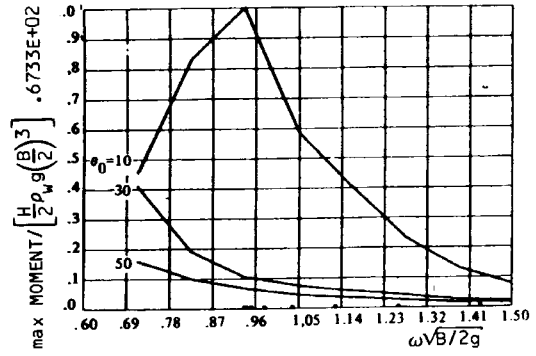
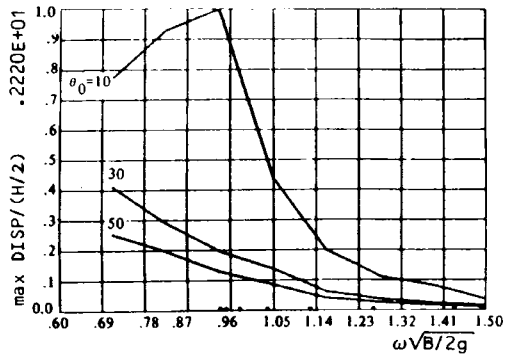


FIG. 9 RAYLEIGH-RITZ APPROXIMATION OF BRIDGE RESPONSE, HEAVE MOTION

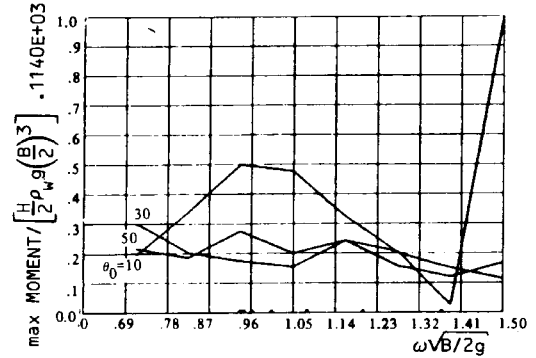
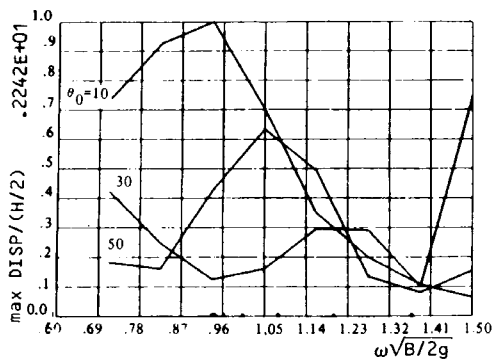


FIG. 10 FINITE ELEMENT I APPROXIMATION OF BRIDGE RESPONSE, HEAVE MOTION

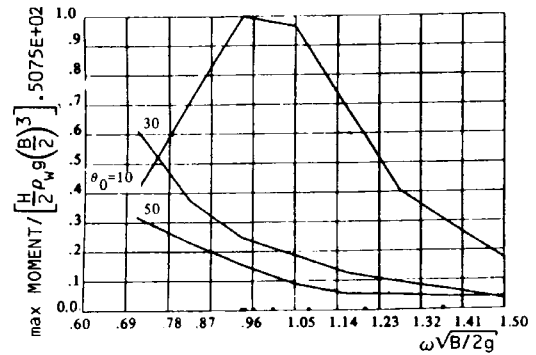
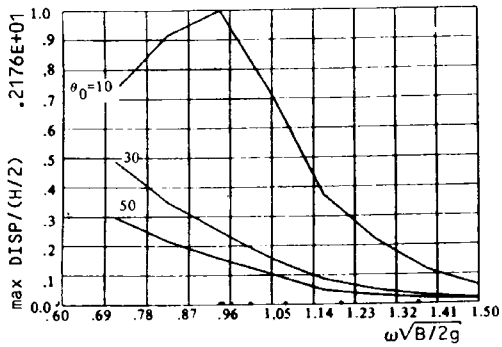


FIG. 11 FINITE ELEMENT II APPROXIMATION OF BRIDGE RESPONSE, HEAVE MOTION

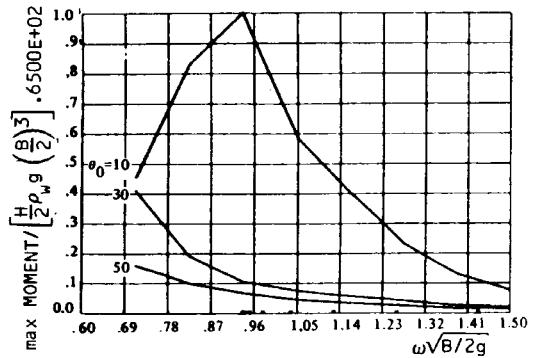
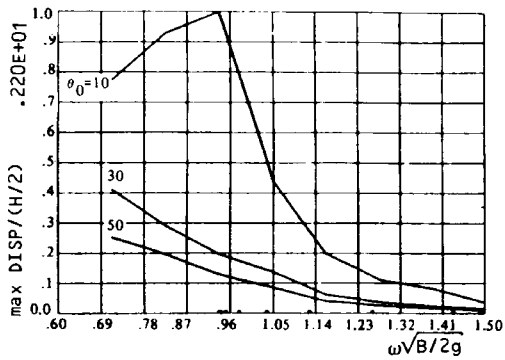


FIG. 12 FINITE ELEMENT III APPROXIMATION OF BRIDGE RESPONSE, HEAVE MOTION

REFERENCES

- 1 Kinsman, B., "Wind Waves, their Generation and Propagation on the Ocean Surface", Prentice Hall, 1965.
- 2 Panicker, N.N., "Review of the Techniques for Directional Spectra", Proc. Int. Symp. on Ocean Wave Measurement and Analysis, ASCE, vol. 1, 1974.
- 3 Borgman, L.E., "Ocean Wave Simulation for Engineering Design", J. ASCE WW4, Nov. 1969, pp 557-583.
- 4 Newman, J.N., "Marine Hydrodynamics", MIT Press, Cambridge Massachusetts, 1980.
- 5 Vugts, J.H. "The Hydrodynamic Forces and Ship Motions", Vitgererij Waltman Delf, 1970.
- 6 Georgiadis, C., "Wave Induced Vibrations of Continuous Floating Structures", Ph.D. dissertation, Univ. of Washington, Seattle, May 1981.
- 7 Blevins, R.D., "Formulas for Natural Frequency and Mode Shape" Van Nostrand Reinhold Co, New York, 1979.
- 8 Georgiadis, C., "Response of Continuous Floating Structures to Infinite Crested Oblique Waves", report, SINTEF, STF71-A82005, Trondheim, Norway, March 1982.
- 9 Zienkiewicz, O.C., "The Finite Element Method", third edition, McGraw-Hill-Co., New York, 1977.
- 10 Hartz, B.J., "Dynamic Response of the Hood-Canal Floating Bridge", Proceedings Second ASCE/EMD Specialty Conference on Dynamic Response of Structures, Atlanta, GA, Jan. 15-16, 1981.

reprinted from

Proceedings of the Third International Offshore Mechanics and Arctic Engineering Symposium -- Volume I

Editor: Jin S. Chung
(Book No. 100171)

published by

THE AMERICAN SOCIETY OF MECHANICAL ENGINEERS
345 East 47th Street, New York, N.Y. 10017
Printed in U.S.A.